This article has been accepted for publication in a future issue of this journal, but has not been fully edited. Content may change prior to final publication. Citation information: DOI 10.1109/JSEN.2014.2341915, IEEE Sensors Journal

Fabric Nanocomposite Resistance Temperature Detector

Nathaniel J. Blasdel, *Member, IEEE*, Evan K. Wujcik, *Member, IEEE*, Joan Carletta, *Senior Member, IEEE,* Kye-Shin Lee, *Member, IEEE*, Chelsea N. Monty

***Abstract*— This paper illustrates the characterization of a fabric resistance temperature detector made from electrospun nylon-6 functionalized with multiwalled carbon nanotubes (MWCNTs) and polypyrrole (PPy) for use in supracutaneous applications like smart clothing, prosthetic sockets, and other medical devices where a temperature detecting fabric is better suited than a rigid detector. The nanocomposite material acts like a resistance temperature detector (RTD), because the conductivity increases linearly with temperature. The empirically determined Temperature Coefficient of Resistance (TCR) is reported for this material, and is –0.204 ± 0.008 %/C. Development of a simple and scalable process for constructing the detector utilized electrospinning nylon-6 as a membrane style substrate, vacuum filtration of MWCNTs onto the nylon scaffold, and vapor phase polymerization of pyrrole to PPy onto the MWCNT functionalized nylon nanofibers. The optimal loading of MWCNTs is 6.6 weight percent. The conductivity of the device follows a percolative behavior and TCR values indicate this is a viable option for temperature detection. Resistance decreases with increasing temperature, which indicates this is a negative TCR material.**

***Index Terms*—Carbon nanotubes, Nanocomposites, Nanotube devices, Temperature sensors**

I. Introduction

Temperature detection close to the skin is normally an easily completed task using a thermometer, but it becomes more difficult when trying to monitor conditions in an enclosed environment around the skin as the detection area, i.e. temperature measurement inside clothing or prosthetics. This is mainly due to the desire for accurate measurements while maintaining comfort, especially for prolonged use or wear. The majority of temperature detectors are made from rigid materials that would create pressure points against the skin in load-bearing situations. This paper discusses a soft fabric thermal sensor modeled after common RTDs to monitor temperature changes at or close to the human skin. This fabric utilizes a nanocomposite material consisting of an insulating nylon-6 substrate functionalized with multiwalled carbon nanotubes (MWCNTs) and polypyrrole (PPy) as the conductive sensing layers.

Manuscript received May 27, 2014; revised July 14, 2014; and accepted July 21, 2014. This work was supported in part by the Wright Center For Sensor Systems Engineering (WCSSE) and Austen BioInnovation Institute In Akron under grant [WCSSE 02-01 (ABIA 10.09.01-01)].

C. N. Monty is with The Department of Chemical And Biomolecular Engineering, The University of Akron, Akron, OH 44325 USA, (phone: 330-972-7255; fax: 330-972-5856; e-mail: cm78@uakron.edu).

N. J. Blasdel is with The Department of Chemical and Biomolecular Engineering, The University of Akron, Akron, OH 44325 USA, (e-mail: njb7@zips.uakron.edu).

E. K. Wujcik is with The Department of Chemical Engineering at Lamar University, Beaumont, TX 77710 USA, (e-mail: Evan.Wujcik@lamar.edu).

J. E. Carletta is with The Department of Electrical and Computer Engineering, The University of Akron, Akron, OH 44325 USA, (e-mail: carlett@uakron.edu).

K.-S. Lee is with The Department of Electrical and Computer Engineering, The University of Akron, Akron, OH 44325 USA, (e-mail: klee3@uakron.edu).

II. Background

Resistance temperature detection is a highly utilized natural material property in which a change in temperature is correlated to the resulting change in resistance of the detector material. Ever since its first use in the mid-19th century by C.W. Siemens, and its refinement by Callendar and Van Dusen in the late 19th century and early 20th century, respectively, resistance temperature detection has become the most widely utilized phenomenon for temperature measurement applications [1]. The resistance, R, for most metals near and above the Debye temperature can be described as a function of the temperature, T, by

$$R = R_0\left(1 + AT + BT^2 + C'T^3\right) \tag{1}$$

where R_0 is the resistance at 0ºC, and A, B, and C' are material constants that are empirically determined [2]. Callendar found that for temperatures above the freezing point of water, the third and fourth terms are unnecessary [2]; at resistances above water's freezing point, and when millikelvin accuracy is not required, the simplified linear model.

$$R \approx R_0\left(1 + \alpha T\right) \tag{2}$$

can be used [2]; in this simplified version, α, which replaces A in the third-order model, is called the TCR. In general, the TCR of a material is defined by

$$\alpha \equiv \frac{1}{R_0}\frac{dR}{dT} \tag{3}$$

This article has been accepted for publication in a future issue of this journal, but has not been fully edited. Content may change prior to final publication. Citation information: DOI 10.1109/JSEN.2014.2341915, IEEE Sensors Journal

This definition can be applied to many different types of resistance-temperature sensing elements, provided an unambiguous relationship between electrical resistance and temperature can be made for the material [2].

RTDs possess a unique quality of having a linear characteristic *R* versus *T* relationship over a rather large range of temperatures. They are most commonly made from pure metals in the form of encapsulated wires, coils, or thin films and typically have positive TCR values, which means that their resistance increases with increasing temperature [2]. Additionally, pure metal RTDs have specific geometric constraints and conformational limitations, and because of the rigidity of their materials of construction, they can be easily damaged and rendered useless; therefore, challenges are faced when trying to miniaturize and protect the sensing elements for use in smart textiles.

Due to these limitations, recent work has focused on the development of CNT temperature sensors, which may meet the configurational needs for temperature detection close to the skin [3]–[8]. Carbon nanotube detectors have emerged for a wide variety of applications due to their excellent mechanical and thermal stability, high thermal and electrical conductivity, and large specific area [9]. Depending on the type of sensor needed, carbon nanotubes have been tailored to sense an array of physical properties, like biological, chemical, flow, gas, mass, optical, position, pressure, stress, strain, and thermal phenomena [9]–[16]. Previously developed carbon nanotube temperature sensors are MEMS-based and have a TCR value in the range of –0.1 to –0.57 %/°C [3]–[7]. The negative TCR value indicates that the material's electrical resistance decreases as its temperature increases.

The sensing material described in this work is composed of nylon-6, an inexpensive high-strength polymer that is commonly used in surgical sutures and toothbrush bristles. Nylon-6 is a chemical resistant polymer possessing a high elastic modulus and is abrasion resistant. This makes it sufficiently tough and durable for use as the sensor substrate. As nylon is also used in some clothing, it is easily spun or woven and altered to fit the size and shape of the desired testing area, and the high surface area and hydrophilicity of nylon nanofibers make it an excellent fabric for use at the surface of the skin [17].

The non-conductive polymer scaffold is functionalized with MWCNTs. The unique properties of MWCNTs offer a superior material for sensing applications and their relatively large conductivity is the reason for using this material as the bulk charge carrier of this detector. Research has also shown that electrospinning MWCNTs into nylon-6 results in a material with a higher tensile strength (+25%), a lower strain at break (-18%), a higher yield stress (+34%), and a higher Young's modulus (~28 MPa) than nylon-6 alone [18]. The functionalized material is also abrasion and chemical resistant, has spatial properties that are easy to manipulate, has large surface area per mass, and is highly permeable.

The nylon-6/MWCNT nanocomposite, in this work, is then functionalized with polypyrrole. Polypyrrole is a conductive polymer that has been shown to respond to temperature and humidity variations, as well as to a range of different gases at various temperatures [19]–[23]. It has been studied as a composite material with carbon nanotubes for a variety of applications, including electrodes in supercapacitors [24], catalyst support material in membrane fuel cells [25], and gas and immunosensors [11], [26], [27]. Polypyrrole is fairly stable, but when exposed to the ambient environmental conditions of air and moisture, it degrades by oxidative processes [26], [27]. This material was chosen because it is temperature sensitive and, with the proper encapsulation to prevent humidity effects, it could be a useful thermal sensor for close to the skin applications.

This paper illustrates the ability of a polymer/CNT nanocomposite thermal sensor to detect temperature changes between 25ºC and 45ºC. One advantage of the material presented in this work is that it responds linearly to a change in temperature in the body-temperature range, making its response more like a RTD than a nonlinearly responding thermistor. This allows for a linear temperature-resistance characteristic, and easier calibrations. This material could be used to monitor the relative environment in prosthetic sockets or smart clothing. The ability of carbon nanotubes to be functionalized with different materials for detection of a wide range of different biological and chemical analytes also shows the potential of the nanocomposite for use in other biomedical and electronics applications [11], [12], [26], [28]–[30]. This paper will address the fabrication and physical characterization of the nanocomposite material, as well as electrical characterization to show the material's response to changing temperature.

III. Experimental

A. Materials

All chemicals and materials were used as received with no further purification. Nylon-6 with a viscosity-averaged molecular weight of 10,000 grams per mole was acquired from Scientific Polymers Inc. (U.S.A.). MWCNTs with diameters in the range of 10 to 20-nanometers and lengths in the range of 0.5 to 2-micrometers were obtained from Nanostructured and Amorphous Materials Inc. (U.S.A.). Triton X-114 (TX-114) surfactant is from Acros Organics (U.S.A) and iron chloride hexahydrate is from Flynn Scientific Inc. (U.S.A.). Pyrrole (≥99%, extra pure), formic acid (98%), and acetic acid (≥99%) were acquired through Sigma Aldrich (U.S.A).

B. Electrospinning

The nylon-6 substrate was electrospun using a homemade cabinet with rotating drum. A World Precision Instruments Inc. (U.S.A.) SP101I syringe pump and a Gamma High Voltage Research (U.S.A.) ES30P-5W voltage source were used. The fibers were spun using a 20% by weight solution of nylon-6 in a 1:1 by weight mixture of formic and acetic acid [17]. The syringe pump flow rate was 9.1-microliters per minute. 25-kilovolts were applied between the needle and collector. The needle to collector distance was 9-centimeters. The collector was a copper sheet encased in a paper towel. It was attached to the rotating drum, which was powered by a variac at a setting of 30-volts to give approximately 7-revolutions per minute. The fiber mats were spun for 4-hours.

This article has been accepted for publication in a future issue of this journal, but has not been fully edited. Content may change prior to final publication. Citation information: DOI 10.1109/JSEN.2014.2341915, IEEE Sensors Journal

C. *Nylon-6 Functionalization*

The nylon-6 fiber mat was cut into multiple 47-millimeter diameter discs for use as membrane style filters. Each membrane was placed into a Fisherbrand™ membrane vacuum filtration funnel. Then it was wet with approximately 1-milliliter of 0.3% TX-114 solution. A 1-gram per liter MWCNT stock solution was made in 0.3% TX-114 and diluted to desired MWCNT concentrations for filtration. TX-114 was used because of the reported enhanced adsorption efficiency of TX-114 for MWCNTs [31]. 250-300 milliliters of this solution were vacuum filtered through the nylon-6 membranes using approximately 17-kilopascals of vacuum. The membranes were washed with deionized water and acetone and allowed to dry before application of 25-millimolar iron chloride hexahydrate solutions. 1 milliliter of the iron chloride solution was applied to the membrane by pipette to fully cover the membrane in solution and left to dry overnight in a desiccator. The membranes were then placed into plastic weigh boats and then, into the polymerization chamber with 1 to 2-milliliters of pyrrole sitting next to them in a beaker. 100-kilopascals of vacuum was applied to the chamber to facilitate pyrrole vaporization. The membranes sat in the pyrrole vapor for 48 hours to complete the polymerization. After polymerization of pyrrole to polypyrrole, the detectors were allowed to sit covered, in air until testing. The material was connected to two copper electrodes using conductive carbon paint. These devices were vacuum-sealed inside kitchen grade vacuum sealing bags, where they were then cut down and vacuum-sealed to final dimensions of approximately 80 millimeters by 20 millimeters.

D. *Detector Testing and Characterization*

Fig. 1 shows a schematic of the detector design. Detector testing and characterization included SEM imaging, TGA, and DC electrical measurements of the polymer nanocomposite in a humidity and temperature-controlled box. SEM imaging utilized a JEOL JSM-7401F (Japan) field emission scanning electron microscope with an accelerating voltage of 1.5-kilovolts and a 13-millimeter working distance. TGA thermographs were acquired using a TA Instruments Q500 thermogravimetric analyzer with a platinum boat at a ramp rate of 10-ºC per minute up to 600-ºC. DC measurements were obtained using a Solartron 1470E (UK) multichannel potentiostat/galvanostat, by applying a 0.7-volt potential and measuring the current while changing the box temperature. The box conditions were controlled using a J-KEM Apollo temperature controller and Omega Engineering HX15 (USA) humidity probe with OM-CP-QUADPROCESS-25MA data logger. The humidity of the box, labeled 2 in Fig. 2, was controlled at 0% RH. The box humidity was measured using the data acquisition system labeled 1 in Fig. 2 in conjunction with the humidity probe inside the box labeled 2 in Fig. 2. Dried air flows through the box at a rate of 400-ccm from the flow meters labeled 4 in Fig. 2 to maintain 0%RH during the tests. The temperature cycles were conducted by the J-KEM temperature controller labeled 3 in Fig. 2 at 30ºC per hour from 25ºC to 45ºC and back down to 25ºC at 15ºC per hour.

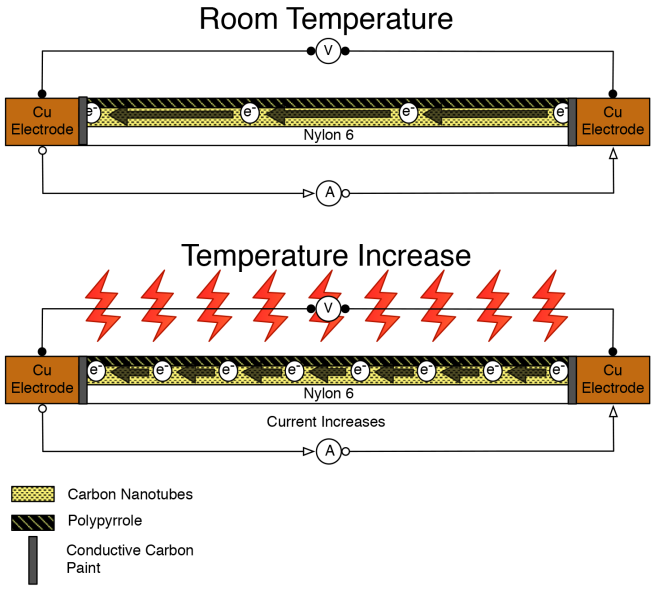

Figure 1. Schematic illustration showing the thermal sensor response, which is described as a decrease in material resistance with increasing temperature.

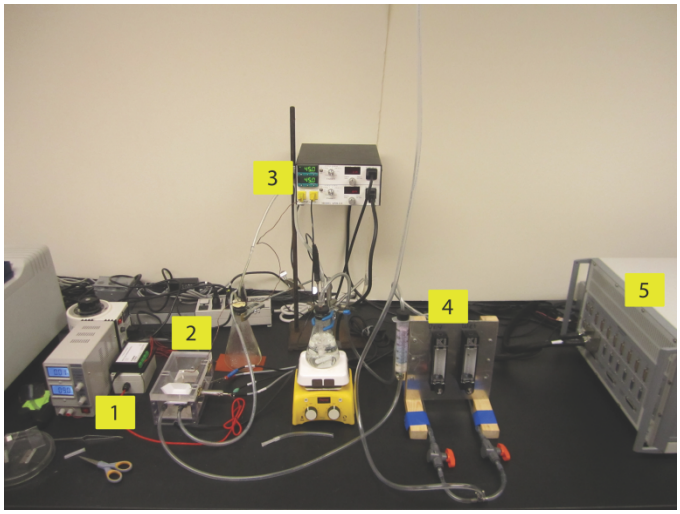

Figure 2. Temperature and humidity controlled sensor-testing system. 1. Omega Engineering HX15 (USA) humidity probe with OM-CP-QUADPROCESS-25MA data logger attached to a computer and variable control power supply. 2. In house fabricated temperature and humidity controlled box with a 75 Watt silicon heating element pad adhered to the aluminum plate, which makes up the bottom of the otherwise polycarbonate box with humid air and dry air inlets and one outlet. 3. JKEM temperature controller attached to a computer for data acquisition with a K-Type thermocouple in the box. 4. Humid air and dry air flow meters for air quality control. 5. DC electrical measurements taken using a Solartron 1470E multichannel potentiostat/galvanostat attached to a computer for data acquisition.

IV. Results and Discussion

A. *Sensor Characterization*

The morphology of the nylon-6/MWCNT/polypyrrole nanocomposite is shown in Fig. 3 as taken by SEM. Fig. 3a shows the bare nylon-6 fibers before functionalization. The nylon-6 fibers range in diameter from 123 to 180-nanometers and the fiber mat porosity ranges from 0.86 to 0.89. Fig. 3b shows the nylon-6 fibers after functionalization with MWCNTs. Notice many of the nanotubes agglomerate into

This article has been accepted for publication in a future issue of this journal, but has not been fully edited. Content may change prior to final publication. Citation information: DOI 10.1109/JSEN.2014.2341915, IEEE Sensors Journal

bundles and lay individually on the nanofibers, creating a disconnected network that leads to high resistances of the matrix before pyrrole polymerization. Fig. 3c shows the polypyrrole coated composite. Polypyrrole polymerization integrates the MWCNT network and allows for higher conductivity and responses that are more sensitive to changing temperature.

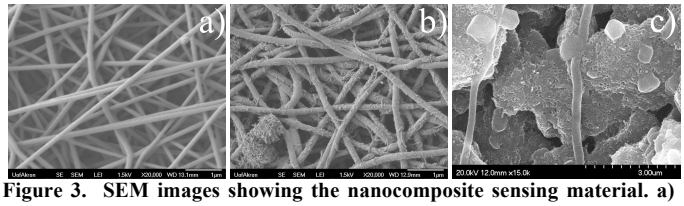

Figure 3. SEM images showing the nanocomposite sensing material. a) neat nylon-6 nanofibers, b) MWCNT functionalized nylon nanofibers, and c) polypyrrole coated composite material.

Thermal gravimetric analysis (TGA) was performed on nanocomposite samples prepared using various concentrations of MWCNTs in the filtration solution, as well as on neat nylon samples, to examine the amount of MWCNTs adsorbed on the nylon nanofiber surface. As hypothesized, the nanocomposites prepared at higher MWCNT filtration concentrations show a higher weight percent of carbon, seen in Fig. 4. This figure shows a characteristic value for the neat nylon samples, as well as normalized (neat nylon baseline subtracted out) values of samples prepared under various filtration conditions. The thermograms in Fig. 4 illustrate that the loading of MWCNTs can be varied during the construction process to ultimately tailor the device resistance.

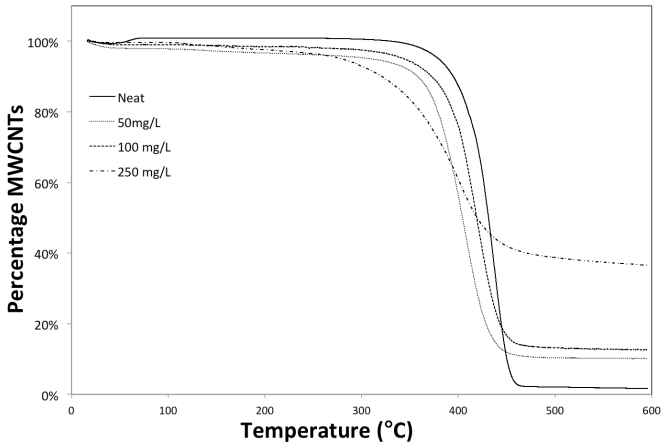

Figure 4. Example TGA thermogram showing the effect that changing the MWCNT concentration in the filtration solution has on the weight percent of nanotubes on the membrane surface.

A typical I-V curve for the nanocomposite material is shown in Fig. 5. The linearity of the I-V curve demonstrates that the material acts as an ideal resistor over the voltage range tested and that there should be very little noise in the resistance data. The linearity of these graphs, along with resistance and sensitivity data, were used to choose the optimum material.

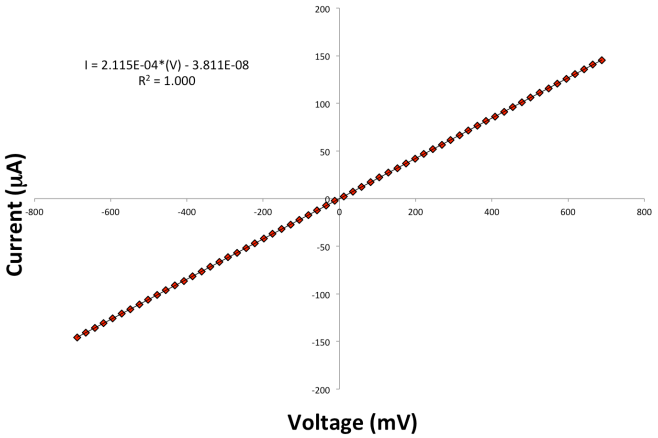

Figure 5. Linear current-voltage characteristic curve of the sensor material from -0.7V to 0.7V.

B. Sensor Evaluation

The resistance of the nanocomposite can be tailored by varying MWCNT loading through the detector construction process. Previous work has shown that the nanocomposite has a percolation threshold of 2% [32], [33]. In this work, the optimum loading was found by determining the alpha values of nanocomposites with increasing MWCNT loadings. Optimum MWCNT loading was determined to be approximately 6.6 weight percent MWCNTs resulting in a TCR (alpha value) of –0.228 ± 0.03%/ºC. This TCR value was calculated as the average of three nanocomposite sensors.

Initial data shows the ability of a nylon-6/MWCNT/PPy nanocomposite to determine changes in temperature. Fig. 6 shows the changing resistance of the RTD when the temperature is changed in 4-degree increments from 25ºC to 45ºC, with three-hour hold times at each temperature. Detector testing was limited to this range in order to correlate practical temperatures potentially seen at the surface of the skin for a variety of conditions [34]–[37]. The diamonds denote the up ramp and the triangles denote the down ramp. The detector resistance is sensitive towards temperature changes and a response is seen immediately upon changing temperature (see inset). This graph shows that the resistance-temperature relationship is highly linear, which makes the nanocomposite a viable thermal sensor candidate.

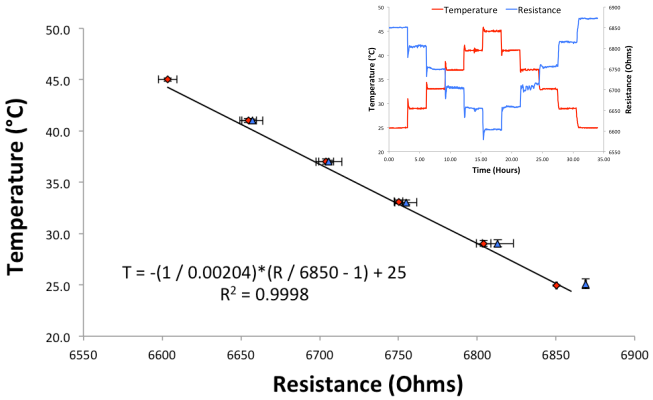

Figure 6. Graph showing the steady state calibration curve data. Red diamonds indicate the up ramp and the blue triangles indicate the down ramp. Inset graph shows the raw data used to calculate the calibrated data points.

This article has been accepted for publication in a future issue of this journal, but has not been fully edited. Content may change prior to final publication. Citation information: DOI 10.1109/JSEN.2014.2341915, IEEE Sensors Journal

The average of 100 steady state temperature cycles, as shown in Fig. 6, was used to determine TCR value (–0.204 ± 0.008%/C) of the optimized sensor material. This TCR value corresponds to previously reported values for CNTs and CNT devices, which can range from – 0.1 to – 0.57%/°C [3]–[5], [7], [8]. This shows that the nanocomposite described in this work maintains the sensitivity of MEMS-based CNT temperature sensors constructed using strictly a polymeric substrate.

Because the relationship between resistance and temperature for this material is linear, *dR/dT* in (3) becomes *ΔR/ΔT*. This equation is then rearranged to predict temperature, *T,* from a measured resistance, *R*:

$$T = -\frac{1}{\alpha}\left(\frac{R}{R_0} - 1\right) + T_0 \qquad (4)$$

where R_0 and T_0 are the baseline resistance and temperature established during a calibration process. Temperature was predicted using (4) based on measured resistance of the optimized nanocomposite sensor during 100 temperature cycles, and compared with a thermocouple control. The results of this comparison are shown in Figs. 7 and 8.

Fig. 7 illustrates the actual and predicted (sensor response) temperatures in time for cycling between 25ºC and 45ºC. This graph is an example of 5-cycles taken from the 100-cycle set of data. The temperature was ramped up at 30ºC per hour and down at 15ºC per hour. The solid (black) line in this graph depicts the temperature calculated from the measured resistance over the 5-cycles. The red symbols correspond to the actual temperature as measured by a thermocouple control. This analysis shows the close fit of the calculated temperature, based on the resistance of the nanocomposite sensor, with the directly measured actual temperature, and verifies the ability of the empirically determined (4) to determine temperatures accurately from measured resistances.

Fig. 8 plots temperature as predicted from the sensor response compared to the actual temperature for the data collected during one hundred temperature cycles of the sensor material. After one hundred cycles, the average percent error in the calculated temperature of the sensor material is approximately 4.29% ± 6.33%. The data displayed no appreciable hysteresis, but over 100 cycles total, there was approximately 300 Ohms of drift in the initial resistance, which stabilized over time to be approximately 6850 Ohms at 25ºC. The sensitivity, or *dR/dT* [2], was consistent over the entire 100 cycle set (–13.49 ± 0.33 Ohms/ºC). This data demonstrates the success of the nanocomposite sensor at determining temperature in an accurate and reproducible manner.

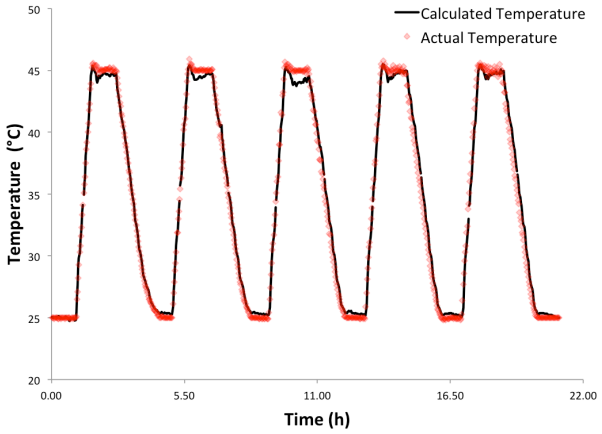

Figure 7. Comparison of the actual temperature and the calculated temperature from (4) using α = -0.204 %/ºC.

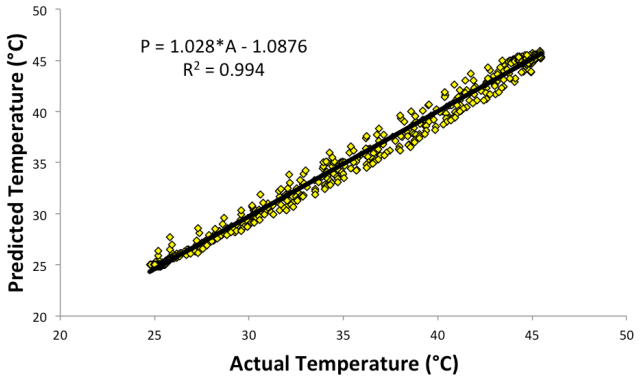

Figure 8. Comparison of the temperature predicted by (4) to the actual recorded temperature.

V. Conclusions

This paper demonstrates the ability of a nylon-6/MWCNT/polypyrrole nanocomposite to act as a reliable RTD in the temperature range of 25ºC to 45ºC. Nanocomposite characterization shows percolation behavior at the material surface, with 6.6 weight percent MWCNTs being the optimal loading. PPy coating enhances the electrical conductivity of the material by interconnecting the MWCNTs. The nanocomposite has an average negative TCR value of –0.204 ± 0.008 %/ºC. This value is comparable to that of previously studied carbon nanotubes and devices, but this sensor is different in that it is made using strictly a polymeric substrate. The material displayed no appreciable hysteresis and the average percent error of the calculated temperature from the recorded temperature was 4.29% ± 6.33% over 100 cycles. This material shows promise for use in monitoring prosthetic socket environments or for other smart clothing applications; however, more research is required to develop this material into a robust sensing device for circuit integration. Continuation of this work will include optimization of the electrospinning parameters including the type and concentration of polymer used in the electrospinning solution, and polypyrrole film formation. It will also include a thorough investigation into humidity and environmental effects on the sensor response.

ACKNOWLEDGMENT

The authors would like to personally thank Dr. Edward Evans of the University of Akron's Department of Chemical and Biomolecular Engineering for his knowledge and laboratory space provided to electrospin our polymer matrix. The authors would also like to acknowledge the undergraduate researchers who helped make this work possible. Thank you, Andrew Thomas, Christopher Alcorn, Christopher King, Christopher Denison, Joshua Schnitzler, Katrina Sedlock, and Marcus Grimm.

REFERENCES

[1] L. B. Hunt, "The Origin of the Platinum Resistance Thermometer," *Platinum Metals Rev.*, vol. 24, no. 3, pp. 104–112, Jul. 1980.

[2] T. D. McGee, *Principles and methods of temperature measurement*. New York: Wiley, 1988.

[3] V. T. Dau, D. V. Dao, T. Yamada, B. T. Tung, K. Hata, and S. Sugiyama, "Integration of SWNT film into MEMS for a micro-thermoelectric device," *Smart Materials and Structures*, vol. 19, no. 7, p. 075003, Jul. 2010.

[4] S. Selvarasah, C.-L. Chen, S.-H. Chao, P. Makaram, A. Busnaina, and M. R. Dokmeci, "A Three Dimensional Thermal Sensor Based on Single-Walled Carbon Nanotubes," in *Solid-State Sensors, Actuators and Microsystems Conference, 2007. TRANSDUCERS 2007. International*, 2007, pp. 1023–1026.

[5] M. De Volder, D. Reynaerts, C. Van Hoof, S. Tawfick, and A. J. Hart, "A temperature sensor from a self-assembled carbon nanotube microbridge," in *Sensors, 2010 IEEE*, 2010, pp. 2369–2372.

[6] C. K. Fung and W. J. Li, "Ultra-low-power polymer thin film encapsulated carbon nanotube thermal sensors," in *Nanotechnology, 2004. 4th IEEE Conference on*, 2004, pp. 158–160.

[7] C. K. M. Fung, V. T. S. Wong, R. H. M. Chan, and W. J. Li, "Dielectrophoretic Batch Fabrication of Bundled Carbon Nanotube Thermal Sensors," *IEEE Transactions On Nanotechnology*, vol. 3, no. 3, pp. 395–403, Sep. 2004.

[8] T. W. Ebbesen, H. J. Lezec, H. Hiura, J. W. Bennett, H. F. Ghaemi, and T. Thio, "Electrical conductivity of individual carbon nanotubes," *Nature*, vol. 382, no. 6586, pp. 54–56, Jul. 1996.

[9] N. Sinha, J. Ma, and J. T. Yeow, "Carbon nanotube-based sensors," *J Nanosci Nanotechnol*, vol. 6, no. 3, pp. 573–90, 2006.

[10] A. Jorio, G. Dresselhaus, and M. S. Dresselhaus, *Carbon nanotubes : advanced topics in the synthesis, structure, properties, and applications*. Berlin ; New York: Springer, 2008.

[11] C. R. Field, J. Yeom, A. Salehi-Khojin, and R. I. Masel, "Robust fabrication of selective and reversible polymer coated carbon nanotube-based gas sensors," *Sensors and Actuators B: Chemical*, vol. 148, no. 1, pp. 315–322, Jun. 2010.

[12] N. Lala, V. Thavasi, and S. Ramakrishna, "Preparation of Surface Adsorbed and Impregnated Multi-walled Carbon Nanotube/Nylon-6 Nanofiber Composites and Investigation of their Gas Sensing Ability," *Sensors*, vol. 9, no. 1, pp. 86–101, 2009.

[13] J. Li, Y. Lu, Q. Ye, M. Cinke, J. Han, and M. Meyyappan, "Carbon Nanotube Sensors for Gas and Organic Vapor Detection," *Nano Letters*, vol. 3, no. 7, pp. 929–933, Jul. 2003.

[14] O. K. Varghese, P. D. Kichambre, D. Gong, K. G. Ong, E. C. Dickey, and C. A. Grimes, "Gas sensing characteristics of multi-wall carbon nanotubes," *Sensors and Actuators B: Chemical*, vol. 81, no. 1, pp. 32–41, Dec. 2001.

[15] T. Ueda, S. Katsuki, K. Takahashi, H. A. Narges, T. Ikegami, and F. Mitsugi, "Fabrication and characterization of carbon nanotube based high sensitive gas sensors operable at room temperature," *Diamond and Related Materials*, vol. 17, no. 7–10, pp. 1586–1589, Jul. 2008.

[16] E. K. Wujcik and C. N. Monty, "Nanotechnology for implantable sensors: carbon nanotubes and graphene in medicine," *Wiley Interdisciplinary Reviews: Nanomedicine and Nanobiotechnology*, vol. 5, no. 3, pp. 233–249, May 2013.

[17] L. V. der S. Bert De Schoenmaker, "Wicking Properties of Various Polyamide Nanofibrous Structures with an Optimized Method," *Journal of Applied Polymer Science*, vol. 120, pp. 305–310, 2011.

[18] M. B. Bazbouz and G. K. Stylios, "The tensile properties of electrospun nylon 6 single nanofibers," *Journal of Polymer Science Part B: Polymer Physics*, vol. 48, no. 15, pp. 1719–1731, Jun. 2010.

[19] A. Sun, Z. Li, T. Wei, Y. Li, and P. Cui, "Highly sensitive humidity sensor at low humidity based on the quaternized polypyrrole composite film," *Sensors and Actuators B: Chemical*, vol. 142, no. 1, pp. 197–203, 2009.

[20] M.-Z. Yang, C.-L. Dai, and D.-H. Lu, "Polypyrrole Porous Micro Humidity Sensor Integrated with a Ring Oscillator Circuit on Chip," *Sensors*, vol. 10, no. 11, pp. 10095–10104, Nov. 2010.

[21] J.-H. Cho, J.-B. Yu, J.-S. Kim, S.-O. Sohn, D.-D. Lee, and J.-S. Huh, "Sensing behaviors of polypyrrole sensor under humidity condition," *Sensors and Actuators B: Chemical*, vol. 108, no. 1–2, pp. 389–392, 2005.

[22] P. N. Bartlett and S. K. Ling-Chung, "Conducting polymer gas sensors part II: response of polypyrrole to methanol vapour," *Sensors and Actuators*, vol. 19, no. 2, pp. 141–150, 1989.

[23] J. J. Miasik, A. Hooper, and B. C. Tofield, "Conducting polymer gas sensors," *Journal of the Chemical Society, Faraday Transactions 1*, vol. 82, no. 4, p. 1117, 1986.

[24] H. Lee, H. Kim, M. Cho, J. Choi, and Y. Lee, "Fabrication of polypyrrole (PPy)/carbon nanotube (CNT) composite electrode on ceramic fabric for supercapacitor applications," *Electrochimica Acta*, 2011.

[25] H.-S. Oh, K. Kim, and H. Kim, "Polypyrrole-modified hydrophobic carbon nanotubes as promising electrocatalyst supports in polymer electrolyte membrane fuel cells," *International Journal of Hydrogen Energy*, vol. 36, no. 18, pp. 11564–11571, Sep. 2011.

[26] P. D. Tam and N. V. Hieu, "Conducting polymer film-based immunosensors using carbon nanotube/antibodies doped polypyrrole," *Applied Surface Science*, 2011.

[27] K. H. An, S. Y. Jeong, H. R. Hwang, and Y. H. Lee, "Enhanced Sensitivity of a Gas Sensor Incorporating Single-Walled Carbon Nanotube–Polypyrrole Nanocomposites," *Advanced Materials*, vol. 16, no. 12, pp. 1005–1009, Jun. 2004.

[28] P. Qi, O. Vermesh, M. Grecu, A. Javey, Q. Wang, H. Dai, S. Peng, and K. J. Cho, "Toward Large Arrays of Multiplex Functionalized Carbon Nanotube Sensors for Highly Sensitive and Selective Molecular Detection," *Nano Letters*, vol. 3, no. 3, pp. 347–351, Mar. 2003.

[29] C. M. Chang and Y. L. Liu, "Electrical Conductivity Enhancement of Polymer/Multi-walled Carbon Nanotube (MWCNT) Composites by Thermally-induced De-functionalization of MWCNTs," *ACS Applied Materials & Interfaces*, 2011.

[30] B. Pradhan, S. K. Batabyal, and A. J. Pal, "Functionalized carbon nanotubes in donor/acceptor-type photovoltaic devices," *Applied Physics Letters*, vol. 88, no. 9, pp. 093106–093106, 2006.

[31] Y. Bai, D. Lin, F. Wu, Z. Wang, and B. Xing, "Adsorption of Triton X-series surfactants and its role in stabilizing multi-walled carbon nanotube suspensions," *Chemosphere*, vol. 79, no. 4, pp. 362–7, 2010.

[32] P. V. Kodgire, A. R. Bhattacharyya, S. Bose, N. Gupta, A. R. Kulkarni, and A. Misra, "Control of multiwall carbon nanotubes dispersion in polyamide6 matrix: An assessment through electrical conductivity," *Chemical physics letters*, vol. 432, no. 4, pp. 480–485, 2006.

[33] E. K. Wujcik, N. J. Blasdel, D. Trowbridge, and C. N. Monty, "Ion Sensor for the Quantification of Sodium in Sweat Samples," *IEEE Sensors Journal*, vol. 13, no. 9, pp. 3430–3436, Sep. 2013.

[34] E. A. Huff, W. R. Ledoux, J. S. Berge, and G. K. Klute, "Measuring residual limb skin temperatures at the skin-prosthesis interface," *JPO: Journal of Prosthetics and Orthotics*, vol. 20, no. 4, p. 170, 2008.

[35] J. T. Peery, W. R. Ledoux, and G. K. Klute, "Residual-limb skin temperature in transtibial sockets," *J Rehabil Res Dev*, vol. 42, no. 2, pp. 147–54, 2005.

[36] D. G. Armstrong, K. Holtz-Neiderer, C. Wendel, M. J. Mohler, H. R. Kimbriel, and L. A. Lavery, "Skin Temperature Monitoring Reduces the Risk for Diabetic Foot Ulceration in High-risk Patients," *The American Journal of Medicine*, vol. 120, no. 12, pp. 1042–1046, Dec. 2007.

[37] S. J. Benbow, A. W. Chan, D. R. Bowsher, G. Williams, and I. A. Macfarlane, "The prediction of diabetic neuropathic plantar foot ulceration by liquid-crystal contact thermography," *Diabetes Care*, vol. 17, no. 8, pp. 835–839, 1994.

Nathaniel J. Blasdel (M'11) was born in Canton, Ohio, October 31st, 1979. He is currently a Ph.D. candidate in the Laboratory of Advanced Sensor and Electrochemical Research (L.A.S.E.R.) at the University Of Akron's Department Of Chemical And Biomolecular Engineering (Akron, Ohio, USA). He will defend and graduate with his Ph.D. in May 2015, He obtained his B.S. in 2010 in chemical engineering from The University Of Akron (Akron, Ohio, USA).

His current work emphasizes the importance of fundamental chemical, material, and system properties on the electrical characteristics of nanocomposite systems for flexible detectors on fabrics, and their role in practical applications.

Evan K. Wujcik (M'13) was born in Warren, RI, USA. He received a B.S. degree in chemical engineering, a M.S. degree in chemical engineering, a B.S. degree in applied mathematics, and a M.B.A. degree in management from The University of Rhode Island, Kingston, RI, in 2008, 2009, 2010, and 2011, respectively. He received his Ph.D. degree in chemical and biomolecular engineering from The University of Akron, Akron, OH, USA, in 2013.

He is currently an Assistant Professor with the Dan F. Smith Department of Chemical Engineering at Lamar University, Beaumont, TX, USA.

He directs the Materials Engineering And Nanosensor (MEAN) Laboratory, which conducts research at the interface of materials science, interfacial science, and bionanotechnology to create novel sensing platforms, nanosensors, biomaterials, and biosensors.

Joan E. Carletta (M'88–SM'13) received the B.S. degree in electrical engineering from the State University of New York, Buffalo, NY, in 1988, and the Ph.D. in computer engineering from Case Western Reserve University, Cleveland, Ohio, in 1996. She is a professor in the Department of Electrical and Computer Engineering at the University of Akron, Akron, Ohio.

Her research interests include analog and digital electronics and real-time digital signal processing on embedded systems.

Kye-Shin Lee (M'02) received the MS degree from Texas A&M University, College Station, in 2002, and the Ph.D. degree from the University of Texas at Dallas, in 2005, both in electrical engineering. Currently, he is an Assistant Professor at Department of Electrical and Computer Engineering, The University of Akron, Akron, OH.

His research interest includes analog integrated circuits, data converters, and sensors.

Chelsea N. Monty received the MS degree in 2005 and the Ph.D. degree in 2009 from the University of Illinois Urbana-Champaign, both in chemical engineering. Currently, she is an Assistant Professor in the Department of Chemical and Biomolecular Engineering, The University of Akron, Akron, OH.

Her research interest includes the development of advanced sensors and electrochemical techniques.